

Physics of the Jagla model as the liquid-liquid coexistence line slope varies

Jiayuan Luo,¹ Limei Xu,^{2,3} C. Austen Angell,⁴ H. Eugene Stanley,¹
 and Sergey V. Buldyrev^{1,5}

¹Center for Polymer Studies and Department of Physics, Boston University, Boston, Massachusetts 02215, USA

²International Center for Quantum Materials, Peking University, Beijing 100871, China

³Collaborative Innovation Center of Quantum Matter, Beijing, China

⁴Department of Chemistry and Biochemistry, Arizona State University, Tempe, Arizona 85287, USA

⁵Department of Physics, Yeshiva University, 500 West 185th Street, New York, New York 10033, USA

(Received 20 August 2014; accepted 11 May 2015; published online 9 June 2015)

The slope of the coexistence line of the liquid-liquid phase transition can be positive, negative, or zero. All three possibilities have been found in Monte-Carlo simulations of a modified spherically symmetric two-scale Jagla model. Since the liquid-liquid critical point frequently lies in a region of the phase diagram that is difficult to access experimentally, it is of great interest to study critical phenomena in the supercritical region. We therefore study the properties of the Widom line, defined in the one-phase region above the critical point as an extension of the coexistence line near which the loci of various response functions extrema asymptotically converge with each other. This phenomenon is predicted by the scaling theory according to which all response functions can be expressed asymptotically in the vicinity of a critical point as functions of the diverging correlation length. We find that the method of identifying the Widom line as the loci of heat capacity maxima becomes unfruitful when the slope of the coexistence line approaches zero in the T - P plane. In this case, the specific heat displays no maximum in the one-phase region because, for a horizontal phase coexistence line, according to the Clapeyron equation, the enthalpy difference between the coexisting phases is zero, and thus the critical fluctuations do not contribute to enthalpy fluctuations. The extension of the coexistence line beyond the critical point into the one-phase region must in this case be performed using density fluctuations. Although the line of compressibility maxima bifurcates into a symmetrical pair of lines, it remains well-defined. We also study how the glass transition changes as the slope of the coexistence line in the T - P plane approaches zero. We find that for the case of positive slopes, diffusivity shows a fragile-to-strong transition upon crossing the Widom line, while for horizontal slope, diffusivity shows the behavior typical for fragile liquids. © 2015 AIP Publishing LLC. [<http://dx.doi.org/10.1063/1.4921559>]

I. INTRODUCTION

The liquid-liquid phase transition (LLPT), defined as a transition between two liquid states of different densities—low density liquid (LDL) and high density liquid (HDL)—has received considerable attention because it is important for our fundamental understanding of the liquid state of matter.^{1–9} The LLPT has been observed or predicted in many systems, such as elemental,^{10,11} ionic,¹² molecular,¹³ and covalent¹⁴ liquids. In some cases, the LLPT terminates at a liquid-liquid critical point (LLCP), which is considered as the source of the thermodynamic and dynamics anomalies in systems such as liquid water, silicon, silica, and germanium.^{3,10,15–20,22,24,25} Thus, the critical phenomena near the LLCP are of crucial importance for the understanding of the anomalous properties in these systems.^{3,4,22,23} However, the detection of the LLCP or the LLPT can be difficult because in many cases the LLCP is buried in the deep supercooled region where crystallization occurs before the LLCP⁴ is reached. In the case of water, for example, it has been hypothesized that the putative LLCP is the cause of water's anomalous behavior,^{3,24,25} but the existence of a LLCP in deeply supercooled bulk water has not been experimentally verified due to crystallization, even though indications of the

existence of the LLCP have been found both in pressure-induced melting experiments²⁶ and in nanoconfined water.²² LLPT was observed in the ultraviscous region by Amann-Winkel *et al.*²¹

According to scaling theory, asymptotically near the critical point all response functions can be expressed in terms of the correlation length.²⁷ In the supercritical region, different response functions display maxima in the one-phase region along constant pressure P paths or constant temperature T paths.^{3,23,28} The loci of different response function maxima in the T - P plane are different, but they converge in the vicinity of the critical point to a single line, called the Widom line.^{3,23,29} Theoretically, the Widom line is defined as the line of zero ordering field $h_1(P, T) = 0$ projected onto the one-phase region of the pressure-temperature (P – T) plane.³⁰ Along this line, the correlation length ξ reaches its maximum as a function of the ordering field h_1 at a constant thermal field $h_2(P, T)$. As the critical point is approached, the magnitude of the response functions increases and, at the critical point, becomes infinite. This fact provides an alternative way of locating the critical point. That is instead of locating the critical point through the coexistence line below the critical temperature T_c , we locate the critical point through the Widom

line in the one-phase region from the supercritical region by tracing the terminal point of the loci of response function maxima.^{3,30–33} Thus, it is important to find a general model system with an accessible LLCPC that permits the detailed examination of the response functions in the vicinity of the LLCPC.

The Jagla model of liquids is a simplified model in which particles interact via a spherically symmetric two-scale potential with both repulsive and attractive ramps.^{3,17,34,35} With a special choice of parameters, the Jagla model has an accessible LLCPC above the melting line,³ allowing us to explore the behavior near the LLCPC in equilibrium liquid states. In this case, the coexistence line between LDL and HDL is positively sloped, which means that when cooled down along the same isobar, the system changes from LDL to HDL. This behavior is opposite to that of water, where experiments²² and simulations²³ show that the coexistence line can be negatively sloped and that an isobaric cooling path transforms the system from HDL to LDL.³

Gibson and Wilding found that by changing the parameters of the Jagla potential, it is possible to reduce the slope of the coexistence line to zero.³⁶ Recently, it was found that a model with continuous symmetric core-softened potential³⁷ displays a LLPT with a slightly negative coexistence line. Another study using a similar potential³⁸ found negatively sloped loci of response function maxima but no LLCPC. In this paper, we use modified Jagla models to investigate the behavior of the Widom line as the slope of the coexistence line changes from positive to horizontal. In Sec. II, we introduce the modified Jagla model and the simulation method. In Sec. III, we present our simulation results. In Sec. IV, we further investigate the relationship between the LLCPC, the Widom

line, and the glass transition (GT) for systems with different coexistence line slopes. In Sec. V, we discuss our results and summarize our study.

II. MODEL AND METHODS

Here we study the two length-scale Jagla model with both repulsive and attractive ramps.³⁴ In this model, particles interact with a spherically symmetric pair potential

$$U(r) = \begin{cases} \infty, & r < a \\ U_A + (U_R - U_A)(b - r)/(b - a), & a \leq r < b \\ U_A(c - r)/(c - b), & b \leq r < c \\ 0, & r \geq c \end{cases} \quad (1)$$

where a is the hard-core distance, b is the soft-core distance, and c is the long-distance attraction cutoff [Fig. 1]; $U_A = -U_0$ is the minimal potential energy reached at soft-core distance $r = b$, and U_R is the potential energy at the top of the repulsive ramp at hardcore distance $r = a$. We implement a family of Jagla potentials with different parameters, simultaneously decreasing b and c —essentially following the Gibson-Wilding procedure,³⁶ the only difference being that we keep U_A constant. The parameters of different models are presented in Table I.

We perform discrete molecular dynamics (DMD) simulations closely following the method described in detail in Ref. 29. As in Ref. 29, we discretize the ramp into a series of step functions but with the position shifted by half of the step length to minimize the difference between the continuous ramps in Eq. (1) and the step function. The discrete Jagla potentials are

$$U_k(r) = \begin{cases} \infty, & r < a \\ U_R, & a \leq r < a + \frac{1}{2}\Delta r_1 \\ U_R - k\Delta U_1, & a + (k - \frac{1}{2})\Delta r_1 \leq r < a + (k + \frac{1}{2})\Delta r_1, \quad 1 \leq k \leq n_1 - 1 \\ U_A, & b - \frac{1}{2}\Delta r_1 \leq r < b + \frac{1}{2}\Delta r_2 \\ U_A + k\Delta U_2, & b + (k - \frac{1}{2})\Delta r_2 \leq r < b + (k + \frac{1}{2})\Delta r_2, \quad 1 \leq k \leq n_2 - 1 \\ 0, & r \geq c - \frac{1}{2}\Delta r_2 \end{cases}, \quad (2)$$

where $n_1 = 60$ and $n_2 = 20$, $\Delta r_1 = (b - a)/n_1$, $\Delta U_1 = (U_R - U_A)/n_1$, and $\Delta r_2 = (c - b)/n_2$, $\Delta U_2 = U_0/n_2$. Note that the number of steps in the potential is approximately two times larger than in Ref. 29. This allows us to minimize the discrepancy between the results of our simulations and the results of Gibson and Wilding.³⁶

We use a as the unit of length, particle mass m as the unit of mass, and U_0 as the unit of energy. The simulation time t is measured in units of $a\sqrt{m/U_0}$, temperature T in units of U_0/k_B , pressure P in units of U_0/a^3 , density $\rho \equiv N/L^3$ in units of a^{-3} , isobaric specific heat C_P in units of k_B , isothermal compressibility K_T in units of a^3/U_0 , and isobaric thermal expansion α_P in units of k_B/U_0 .

Our results are based on simulations of a liquid system of $N = 1728$ molecules with periodic boundary conditions. Constant volume-temperature (NVT) and constant pressure-temperature (NPT) simulations are implemented in this study. We perform NVT simulations for systems with different number densities with a step of approximately 0.005. Each state point is equilibrated for at least 10^5 time units or if necessary for a longer time such that the root mean square displacement of the particles is at least $3a$. The initial 20% of each run is skipped in order to exclude the non-equilibrated part of the trajectory. We use the NVT simulations to obtain the isotherms near the critical points in order to precisely determine the critical point parameters and to perform the equal area Maxwell

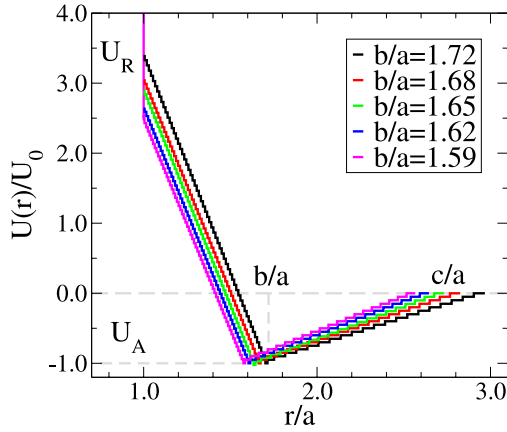


FIG. 1. Family of modified spherically symmetric two-scale Jagla ramp potentials [Table I]. The two length scales of Jagla potential are the hard-core distance $r = a$ and soft-core distance $r = b$. The long range cutoff is $r = c$. We keep the potential minimum U_A constant, and its depth serves as the unit of energy $U_0 = |U_A|$, while the hard-core potential U_R varies. This convention is different from Ref. 36, in which U_R is kept constant $U_R = 0.69U_0$. The discretized versions of the modified Jagla potential from $b/a = 1.72$ to 1.59 are shown. We use different numbers of discretization steps, $n_1 = 60$ for $a \leq r < b$ and $n_2 = 20$ for $b \leq r < c$.

construction for finding the equilibrium pressure $P_e(T)$ below the critical point. Differentiating $P_e(T)$ with respect to T by calculating the finite difference with $\Delta T = 0.005$, we determine the slope of the coexistence line in the vicinity of the critical point. We use the NPT simulations to compute volume V and potential energy U as functions of temperature at constant pressure with temperature step $\Delta T = 0.01$ and pressure step $\Delta P = 0.02$. The isothermal compressibility K_T is calculated by using finite difference as

$$K_T(P, T) = -2 \frac{V(P + \Delta P/2, T) - V(P - \Delta P/2, T)}{[V(P + \Delta P/2, T) + V(P - \Delta P/2, T)]\Delta P}.$$

Similarly, the isobaric thermal expansion coefficient α_P is calculated by using finite difference as

$$\alpha_P(P, T) = 2 \frac{V(P, T + \Delta T/2) - V(P, T - \Delta T/2)}{[V(P, T + \Delta T/2) + V(P, T - \Delta T/2)]\Delta T}.$$

We calculate the isobaric specific heat $C_P(P, T)$ by computing the enthalpy per particle $H = (U + PV)/N$ omitting the trivial kinetic contribution $3/2K_B T$ and using finite difference

$$C_P(P, T) = \frac{H(P, T + \Delta T/2) - H(P, T - \Delta T/2)}{\Delta T}.$$

The temperature of the system is controlled by the Berendsen thermostat³⁹ which rescales the velocities of all particles

in the NVT simulations so that the average kinetic energy per particle approaches the desired value $3K_B T_0/2$, where T_0 is the temperature of the thermostat,

$$T' = \bar{T}(1 - \kappa_T \tau_t) + T_0 \kappa_T \tau_t, \quad (3)$$

where $\kappa_T = 0.2 [\sqrt{m/U_0}/a]$ is a heat exchange coefficient, τ_t is the time interval between two successive rescalings, T' is the new temperature, and \bar{T} is the average temperature during the time interval τ_t . We select τ_t as the time during which N collisions between particles occur.

For the NPT simulations, the Berendsen barostat algorithm rescales the coordinates \vec{r}_j and box dimensions \vec{L} after each τ_p unit of time,

$$r'_j = r_j + r_j \kappa_p (\bar{P} - P_0), \quad (4)$$

$$\vec{L} = \vec{L} + \vec{L} \kappa_p (\bar{P} - P_0), \quad (5)$$

where P_0 is the desired pressure, \bar{P} is the average pressure during time interval $\tau_p = 1000\tau_t$, and $\kappa_p = 0.02[a^3/U_0]$ is the rescaling coefficient.

To calculate diffusivity, we first perform simulations at constant pressure using the NPT-ensemble and then compute diffusivity D using the standard Einstein relation based on the mean square displacement of particles shown in Ref. 29, Eq. (5). The diffusion coefficient is usually computed using the NVT-ensemble with the volume of the system artificially restricted to the box of given linear dimensions L_1, L_2 , and L_3 under periodic boundaries. As a result, the density fluctuations on the scales comparable to the box size do not contribute to the displacement of particles. On the other hand, in the NPT-ensemble, the displacement of the particles is affected by the periodic rescaling of the box size. However, for small κ_p , the effect of this rescaling is negligible. Moreover, the size of the simulation box in NPT simulations changes over time and hence the density fluctuations behave more physically than in NVT. To compute the mean displacements of the particles in the periodic box with changing dimensions, we rescale the coordinate of each particle i along direction j by the box size $\tilde{r}_{ij} = r_{ij}/L_j$ and then trace the displacements $\Delta\tilde{r}_{ij}(\tau) = \tilde{r}_{ij}(t + \tau) - \tilde{r}_{ij}(t)$ of each particle using periodic boundaries with a unity box. Next, we compute $\tilde{\Delta}_j(\tau) = \langle [\Delta\tilde{r}_{ij}(\tau)]^2 \rangle$ averaged over all particles in the system and all initial times t . The total mean square displacement of the particles, $\Delta(\tau)$, is given by $\Delta(\tau) = \sum_{j=1}^3 \langle L_j^2 \tilde{\Delta}_j(\tau) \rangle$. By plotting $\Delta(\tau)$ versus τ and finding its least liner fit slope S , we compute the diffusion coefficient using Einstein relation $D = S/6$. We compare the values of diffusivity obtained at constant pressure with those

TABLE I. Renormalized parameters for modified Jagla potential³⁶ along with the values of the critical temperature T_C , pressure P_C , and density ρ_C of the LLCPC obtained for these sets of parameters.

b/a	c/a	U_R/U_0	T_C	P_C	ρ_C
1.72	3.000	3.478	0.386 ± 0.005	0.173 ± 0.005	0.375 ± 0.005
1.70	2.93	3.293	0.352 ± 0.005	0.210 ± 0.005	0.380 ± 0.005
1.68	2.86	3.126	0.322 ± 0.005	0.257 ± 0.005	0.385 ± 0.005
1.65	2.76	2.906	0.271 ± 0.005	0.334 ± 0.005	0.392 ± 0.005
1.62	2.67	2.715	0.243 ± 0.005	0.444 ± 0.005	0.399 ± 0.005
1.60	2.62	2.601	0.232 ± 0.005	0.541 ± 0.005	0.403 ± 0.005
1.59	2.59	2.547	0.226 ± 0.005	0.589 ± 0.005	0.406 ± 0.005

obtained at constant volume for several state points close to the glass transition and find no significant difference.

We perform cooling or heating simulations at a constant cooling/heating rate, $q \equiv \Delta T/\Delta t$, where T decreases/increases by ΔT over time Δt . We perform our simulations at $q = 10^{-6}q_0$ where $q_0 = \sqrt{U_0^3/(ma^2k_B^2)}$. To relate our cooling/heating rate to experimental values for water, we use $a = 0.27$ nm, $U_0 = 4.75$ kJ/mol and $m = 36$ g/mol.¹⁷ For such a set of parameters, $q_0 = 7.7 \times 10^{14} \approx 10^{15}$ K/s.

III. SIMULATION RESULTS

A. The slope of the coexistence line

We first explore the phase diagram of each model with different b/a via slow cooling using constant volume simulations. Figure 2(a) shows the temperature of maximum density (TMD) line, which is the locus of state points at which pressure reaches a minimum along each isochore as a function of T ,²⁹ and the LLCP, which is preliminary determined as the highest temperature crossing of isochores in the T - P phase diagram.²⁹ We then produce a set of NVT simulations in the vicinity of the critical point to obtain a set of isotherms and detect the parameters of the LLCP by finding the inflection points of the isotherms and making a linear interpolation between nearby isotherms to find the T_C , P_C , and ρ_C for which $(\partial P/\partial \rho)_T = 0$ at the inflection point defined by the minimum $(\partial P/\partial \rho)_T$ (see Table I). It shows that the LLCP monotonically shifts to lower temperature and higher pressure as b/a decreases [Fig. 2(a)]. The region of the density anomaly (the region bounded by the TMD line) expands and shifts together with the LLCP to higher pressures as b/a decreases. This coincides with previous results reported in Ref. 36. We note that the numerical differences in P and T arise from the fact that we define the unit of energy as $U_0 \equiv -U_A$, while Ref. 36 uses $U_0 \equiv U_R/0.69$. For $b/a < 1.59$, we are unable to obtain the LLCP and coexistence line due to spontaneous crystallization near the LLCP within a short simulation time.

Using the equal area Maxwell construction for subcritical isotherms, we find the equilibrium pressure $P_e(T)$ and calculate the slope of the LLPT coexistence line dP_e/dT for systems with different b/a [Fig. 2(b)] in the vicinity of the critical point. We find that the slope of the coexistence line does not significantly change in the temperature region below the critical point between $0.9T_C$ and T_C .

One can see that the slope decreases from positive to approximately zero as b/a decreases to 1.59, in agreement with Ref. 36. For large values of b/a , the LLCP lies clearly above the density anomaly region bounded by the TMD line, corresponding to the case of $dP/dT > 0$, while for $b/a = 1.59$, the LLCP lies on the TMD line corresponding to the case of $dP/dT = 0$ [Fig. 2(a)]. Theoretically, if $dP/dT < 0$, the LLCP should be inside the density anomaly region.⁴¹ For the detailed discussion of these facts, see Sec. V.

B. Widom line

For the first-order phase transition, the order parameters (entropy or density) are discontinuous on crossing the coexistence line. At the critical point where the coexistence line terminates, the response functions such as specific heat (C_P), isothermal compressibility (K_T), and isobaric expansion coefficient (α_P) diverge. In the supercritical region, these response functions show maxima in the one-phase region. In this section, we study the behavior of C_P maxima, K_T maxima, and α_P maxima lines near the LLCP for models with different slopes of coexistence line.

1. Isobaric specific heat C_P

Figure 3 shows the behavior of C_P upon cooling along constant pressure for modified Jagla models with different values of $b/a = 1.72, 1.70, 1.68, 1.65, 1.62, 1.59$. Below the critical pressure $P < P_c$, C_P monotonically increases upon cooling in the entire domain of the LDL phase, which becomes metastable for temperatures below the coexistence line. However, above the critical pressure P_c in the one-phase region, we

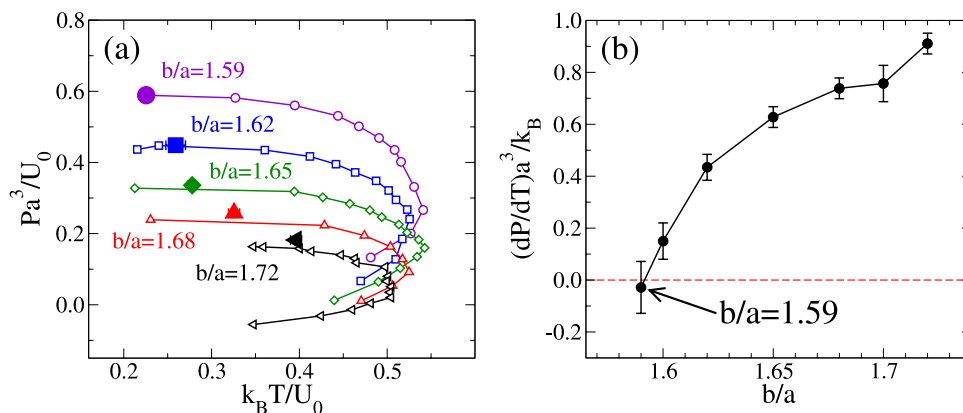


FIG. 2. The LLCP, TMD line, and the slope of the LDL-HDL coexistence line for a selection of modified Jagla potentials. (a) The critical point (solid symbols with error bar approximately the symbol size) and the TMD line (open symbols) for systems with $b/a = 1.72, 1.68, 1.65, 1.62, 1.59$. One can see that the LLCP monotonically shifts to higher pressure and lower temperature as b/a decreases. The density anomaly region bounded by the TMD line expands in the T - P diagram with decreasing b/a , and the LLCP moves from above the TMD line towards the density anomaly region and for $b/a = 1.59$, the LLCP locates right on the TMD line. (b) The slope of the LDL-HDL coexistence lines decreases as the b/a value decreases. When b/a approaches 1.59, the slope decreases to zero.

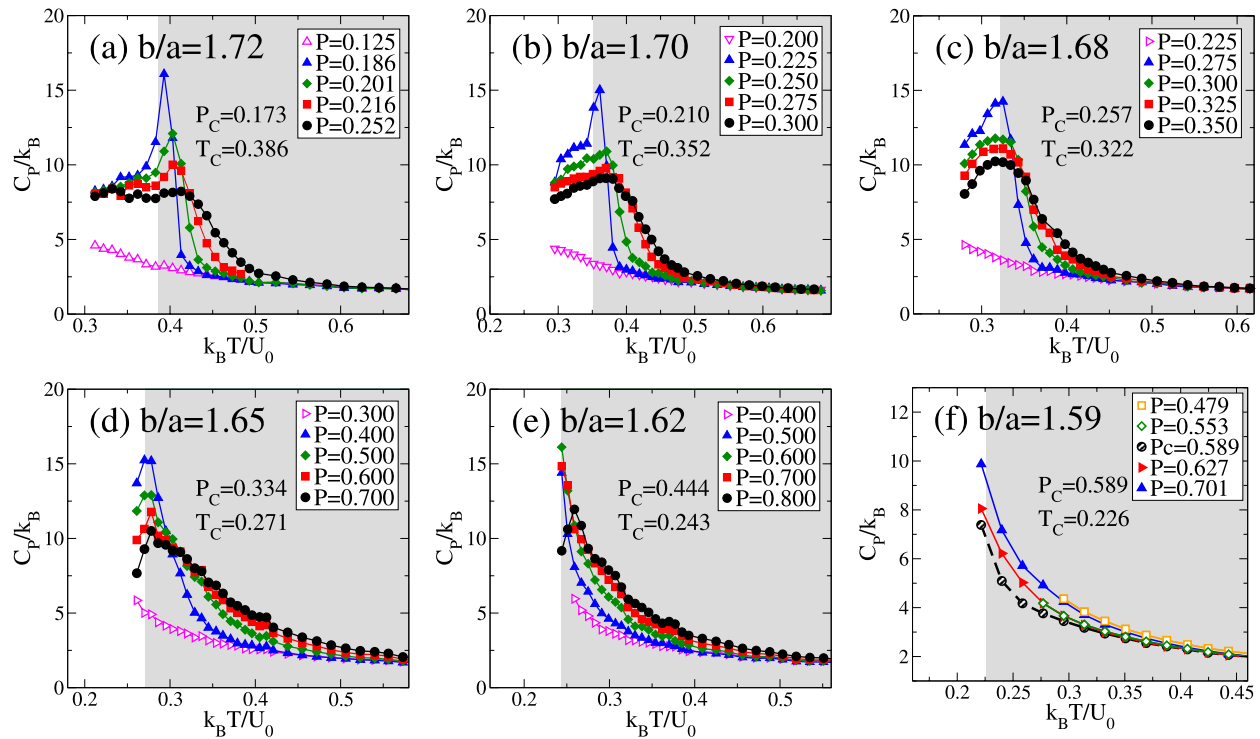


FIG. 3. Specific heat C_P for systems with different b/a . Only equilibrated results are shown. The gray area indicates the $T > T_c$ region. ((a)-(d)) For $b/a \geq 1.65$, one can see that C_P shows maxima at pressures $P > P_c$, and as P_c is approached, the increase in C_P starts at lower T but becomes sharper. As the pressure increases, the C_P peak moves to higher T , indicating a positive slope of the C_P maxima locus, which follows the coexistence line for these models. For pressure $P < P_c$, C_P monotonically increases without any maximum. (e) For $b/a = 1.62$, C_P monotonically increases without showing any peak also for $P > P_c$, except at the highest pressure studied $P = 0.800$. The system enters a glassy state at lower T where no equilibrium data can be obtained. (f) For $b/a = 1.59$ with horizontal coexistence line, no C_P maxima can be found for the equilibrium states with $T \geq T_c$ for both $P > P_c$ and $P < P_c$.

find that C_P shows maxima for $b/a > 1.65$ [Figs. 3(a)–3(d)]. The magnitude of the C_P peaks increases as the LLC is approached from the supercritical region and diverges at the LLC in an infinite system. This suggests that we can locate the LLC by tracing the terminal point of the C_P maxima line.

We note that the C_P peaks move toward higher T at higher P [Figs. 3(a) and 3(b)], indicating a positively sloped locus of C_P maxima. For these values of b/a , the coexistence line is positively sloped, suggesting that the Widom line is the extension of the coexistence line into the one-phase region. However, the slopes of the C_P maxima lines increase as the slopes of the coexistence lines decrease and eventually, at $b/a = 1.65$, the C_P maxima line becomes nearly vertical, clearly showing that the C_P maximum is no longer serving its original purpose, as will be explained in Sec. IV below. For $b/a = 1.62$, C_P monotonically increases without showing any peak for pressures $P > P_c$, except at the highest pressure studied $P = 0.800$ [Fig. 3(e)]. For smaller P , we would expect to find the maximum at $T \approx T_c$, but we were not able to equilibrate the system significantly below T_c in order to observe the decrease of C_P upon cooling. When $b/a = 1.59$ with a horizontal coexistence line, C_P monotonically increases with decreasing T along a constant pressure path both below and above P_c [Fig. 3(f)]. There are no C_P maxima in the equilibrium region with $T \geq T_c$, but C_P behaves symmetrically either below or above P_c .

We plot the lines of equal C_P for two extreme cases, $b/a = 1.72$ with a positively sloped coexistence line [Fig. 4(a)]

and $b/a = 1.59$ with a horizontal coexistence line [Fig. 4(b)]. These lines show the topographic map depiction of the $C_P(T, P)$ landscape in the $(P - T)$ plane. The lines of the specific heat maxima as function of temperature at constant pressure cross the lines of equal C_P at their highest pressure. When $b/a = 1.72$, the lines of equal C_P form loops in the $T - P$ plane and cross the C_P maxima line at the points of their maxima. The locus of C_P maxima extends the coexistence line into the one-phase region in the vicinity of the critical point. Then it sharply turns upwards to higher pressures and becomes approximately vertical. For $b/a = 1.59$, there are no C_P maxima. The equal C_P lines extend away from the critical point symmetrically without any loop. At low T , we reach the simulation limit either due to crystallization for $P < P_c$ or due to entering a glassy state for $P > P_c$, where no equilibrium results can be obtained for the analysis.

We note that the magnitude of C_P drops significantly when the coexistence line is horizontal for $b/a = 1.59$, compared to that for $b/a = 1.72$. This is because, when the coexistence line is horizontal, the difference in entropy S between LDL and HDL is zero according to the Clapeyron equation of thermodynamics,

$$\frac{dP}{dT} = \frac{\Delta S}{\Delta V}. \quad (6)$$

In this case, the entropy fluctuations that determine the magnitude of the specific heat $C_P = \langle (\delta S)^2 \rangle / k_B$ gain no strength from the critical fluctuations.

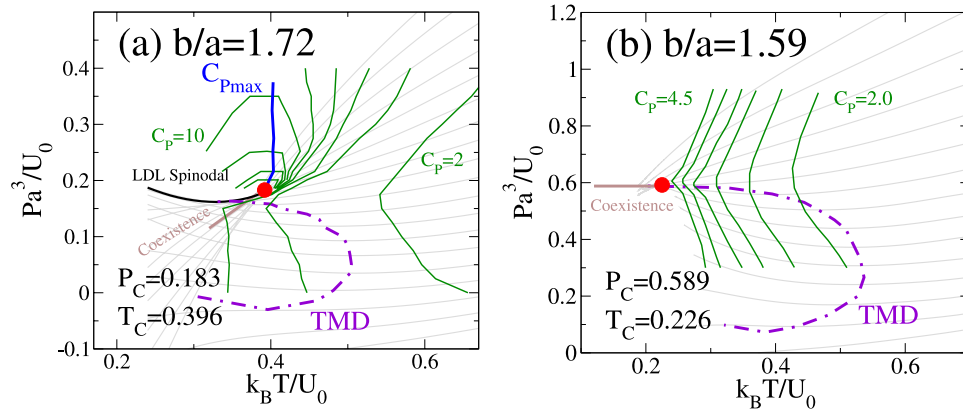


FIG. 4. Lines of equal C_P (solid green). (a) For $b/a = 1.72$, the lines of equal C_P change from $C_P = 2$ far away from the LLC to $C_P = 10$ close to the LLC with an interval of $\Delta C_P = 1$. The loci of C_P maxima cross the lines of equal C_P at the points of their maximal pressure, and follows the coexistence line into the one-phase region, then sharply turns upwards to higher pressures and becomes almost vertical. (b) For $b/a = 1.59$, the lines of equal C_P (solid green) change from $C_P = 2.0$ far away from the LLC to $C_P = 4.5$ close to the LLC with interval $\Delta C_P = 0.5$. No C_P maxima can be observed before the system either goes into glassy states or crystallizes. However, one notes that the C_P is symmetric with respect to the critical pressure.

2. Isothermal compressibility K_T

Figure 5 shows the behavior of K_T above and below P_c . For $b/a \geq 1.62$, when the coexistence line slope is positive, K_T shows maxima both above and below P_c . For $P > P_c$ in the one-phase region, similar to that of C_P , the K_T peak becomes more prominent as the LLC is approached [Figs. 5(a)–5(e)] until it diverges at the LLC for an infinite system. For $P < P_c$, we observe a second set of K_T peaks with much lower magnitudes. For $b/a = 1.59$ with a horizontal coexistence line, K_T

behaves symmetrically in the vicinity of the critical point above and below P_c , with equal magnitudes of the maxima [Fig. 5(f)]. In the case of horizontal slope, the critical region in which the critical density fluctuations are much larger than the background fluctuations is very small. Figure 5(f) shows that K_T for $P = 0.675$ has two maxima: one at $T = 0.27$ corresponding to the critical fluctuations and another at $T = 0.225$ corresponding to the background fluctuations. This causes the high-pressure branch of the K_T maximum line to switch to the maximum of the background fluctuations which become larger

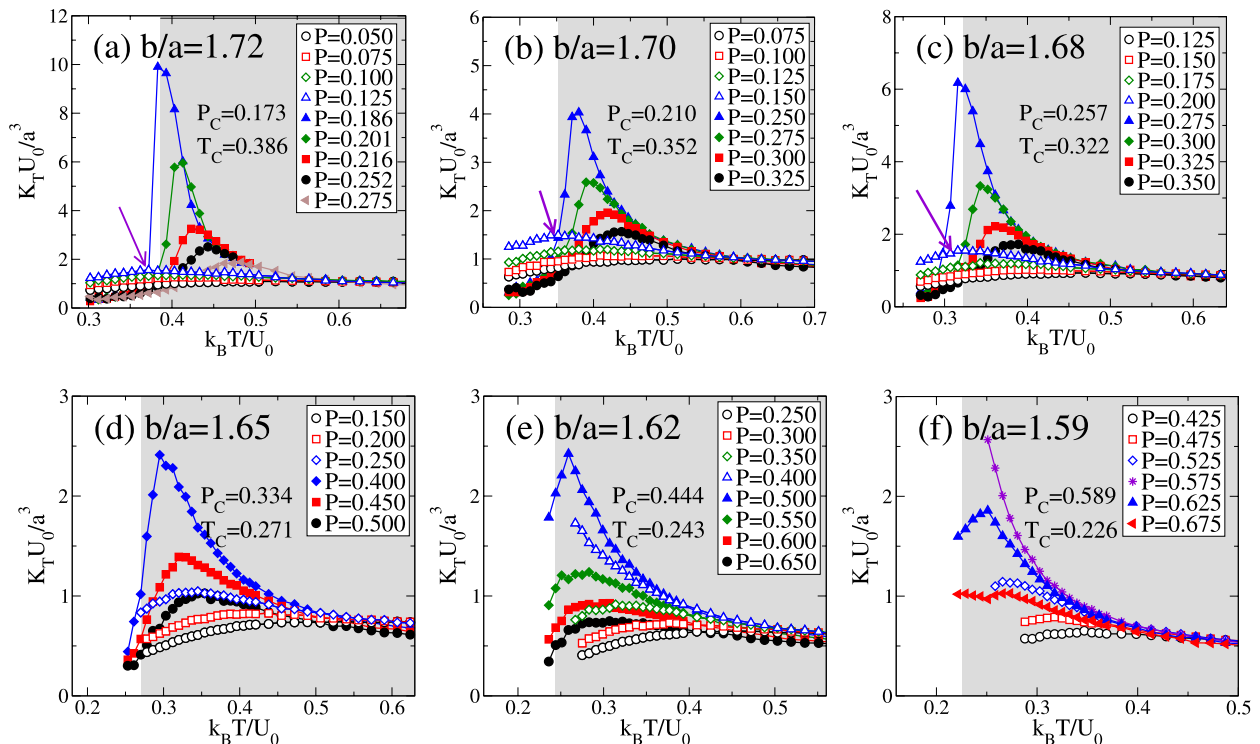


FIG. 5. Compressibility K_T for models with different b/a . The gray area indicates the $T > T_c$ region. The maxima in K_T both for $P < P_c$ (open symbols) and for $P > P_c$ (solid symbols with arrows pointing to the peaks) are shown. ((a)–(e)) For $b/a \leq 1.62$, the magnitudes of K_T for $P > P_c$ are much larger than for $P < P_c$. The maxima for $P > P_c$ correspond to critical fluctuations, while the maxima for $P < P_c$ correspond to the approach to the LDL spinodal. (f) For $b/a = 1.59$, with the horizontal coexistence line, the K_T below and above P_c are almost identical, with equal magnitudes of their maxima. The critical isochore is indicated by a black thin line.

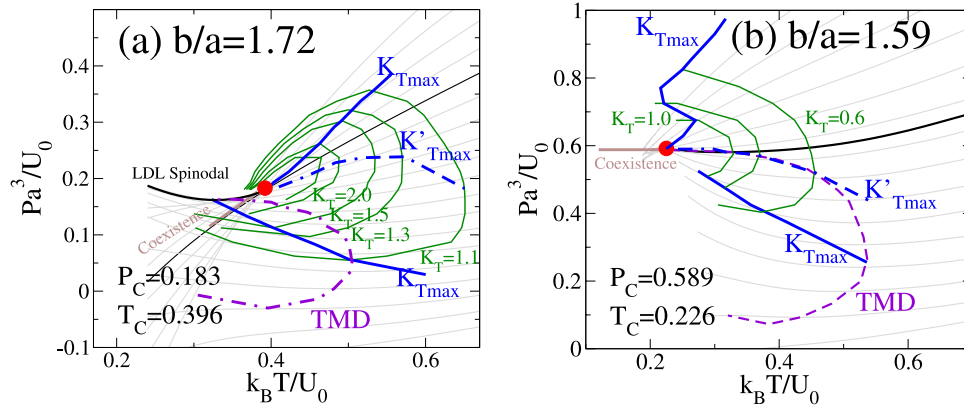


FIG. 6. Lines of equal K_T (solid green). (a) For $b/a = 1.72$, the lines of equal K_T are from $K_T = 1.1$ (far away from the LLC), $K_T = 1.3$, $K_T = 1.5$, $K_T = 2.0$, and $K_T = 2.5$ (close to the LLC). One can see that the loci of the two K_T maxima cross the lines of equal K_T at points of their maximal and minimal pressures and are not symmetric with respect to P_c . The locus with higher magnitude of K_T maxima, which corresponds to the critical fluctuations, merges to the LLC. The locus with the lower magnitude of K_T maxima extends below T_c and terminates at the minimum pressure point of the LDL spinodal, where the TMD line also terminates. This branch of K_T maxima also crosses the TMD line at the point of its maximal temperature. (b) For $b/a = 1.59$, the lines of equal K_T (solid green) change from $K_T = 0.6$ far away to $K_T = 1.0$ close to the LLC with interval $\Delta K_T = 0.2$. The loci of equal K_T form symmetric loops around the LLC, and both K_T maxima lines merge to the LLC with equal magnitudes of their maxima. We also show the K'_{Tmax} line which is the line of K_T maxima as function of pressure at constant temperature, which is almost horizontal and closely follows the critical isochore. It connects the points of maximal temperature on the lines of equal K_T .

than the maximum due to critical fluctuations for $P > 0.675$ [Figure 6(b)].

Figure 6 shows the loci of K_T maxima for both $b/a = 1.72$ with a positive coexistence line slope and $b/a = 1.59$ with a horizontal coexistence line. For $b/a = 1.72$, the values of the K_T maxima at $P > P_c$ correspond to the critical fluctuations, which originate from the LLC. It has a much larger magnitude than the values of the second K_T maxima at $P < P_c$ which corresponds to the approach to the LDL spinodal and terminates at the lowest pressure point of the LDL spinodal where the TMD line also terminates.^{24,40} Furthermore, the K_T maxima line at $P < P_c$ also crosses the TMD line at the point of its maximal temperature.⁴¹ Similar to that of C_p , the lines of equal K_T form loops and cross at their pressure *extrema* with the two branches of K_T maxima lines. For $b/a = 1.59$ [Fig. 6], the lines of equal K_T form symmetric (with respect to P_c) loops around the critical point. Both K_T maxima lines would merge at the LLC but the low-pressure branch of K_T maxima line cannot be reliably traced in the close vicinity of the critical point, because the density fluctuations cause spontaneous crystallization in the vicinity of the maxima of K_T .

3. Isobaric thermal expansion α_P

Figure 7 shows the thermal expansion α_P for systems with different b/a varying from 1.72 to 1.59. In each case for $b/a = 1.72 - 1.59$, $\alpha_P > 0$ for $P > P_c$, while $\alpha_P < 0$ for $P < P_c$ below the TMD. For $b/a \geq 1.62$ with positively sloped coexistence line [Figs. 7(a)–7(e)], the magnitude of the α_P maxima increases as P_c is approached, similar to that of C_p [Fig. 3]. For $b/a = 1.59$ with horizontally sloped coexistence line [Fig. 7(f)], α_P behaves almost symmetrically above and below P_c , with $\alpha_P = 0$ for $P = P_c$, consistent with the theoretical explanation of α_P in terms of fluctuations, $\alpha_P = \langle(\Delta S \Delta V)\rangle/k_B T V$, where $\delta S = \delta H/T = 0$ when the slope of the coexistence line is horizontal.

As can be seen from the equal α_P lines shown in Figure 8, both the positive and negative α_P form loops that are separated

by the TMD line, loci of $\alpha_P = 0$. When the slope of the coexistence line is positive, e.g., for $b/a = 1.72$ [Fig. 9(a)], the α_P maxima line lies between the loci of C_p maxima and K_T maxima, and the α_P minima line meets the lower branch of K_T maxima line at the point of lowest pressure in the LDL spinodal. When the slope of the coexistence line is horizontal, e.g., for $b/a = 1.72$ [Fig. 9(b)], the lines of α_P maxima and minima are almost symmetric with respect to $P = P_c$, with $\alpha_P = 0$ for $P = P_c$ close to the LLC.

4. Diffusivity

As follows from Adam-Gibbs relation,⁴² the sharp C_p maximum as function of T near the critical point is associated with an increase of the absolute value of the slope of the Arrhenius plot of diffusivity.⁴³ Furthermore the sharp decrease of the C_p upon crossing of the Widom line is associated with the subsequent decrease in the slope or at least the restoration of the linearity of the Arrhenius plot at lower temperature. Such kind of behavior is known as fragile to strong transition.⁴³ Indeed, Fig. 10(a) shows such behavior of the diffusivity for the Jagla model with the positive slope of the coexistence line ($b/a = 1.72$). In contrast, in the absence of the C_p maxima ($b/a = 1.59$), the fragile to strong transition cannot be observed [Fig. 10(b)]. In this case, the slope of the Arrhenius plot monotonically decreases upon cooling, as one would expect for a fragile liquid approaching its glass transition.

5. Relation between the Widom line and the critical point

Based on the behaviors of the response functions shown in Figs. 4, 6, and 8, we can identify the Widom line as follows. For systems with positively sloped coexistence line, e.g., $b/a = 1.72$, the Widom line can be determined as the segment where the C_p , K_T , and α_P maxima overlap each other. It is an extension of the coexistence line into the one-phase region in the vicinity of the LLC. In contrast, for systems with horizontally sloped coexistence line, e.g., $b/a = 1.59$, the C_p

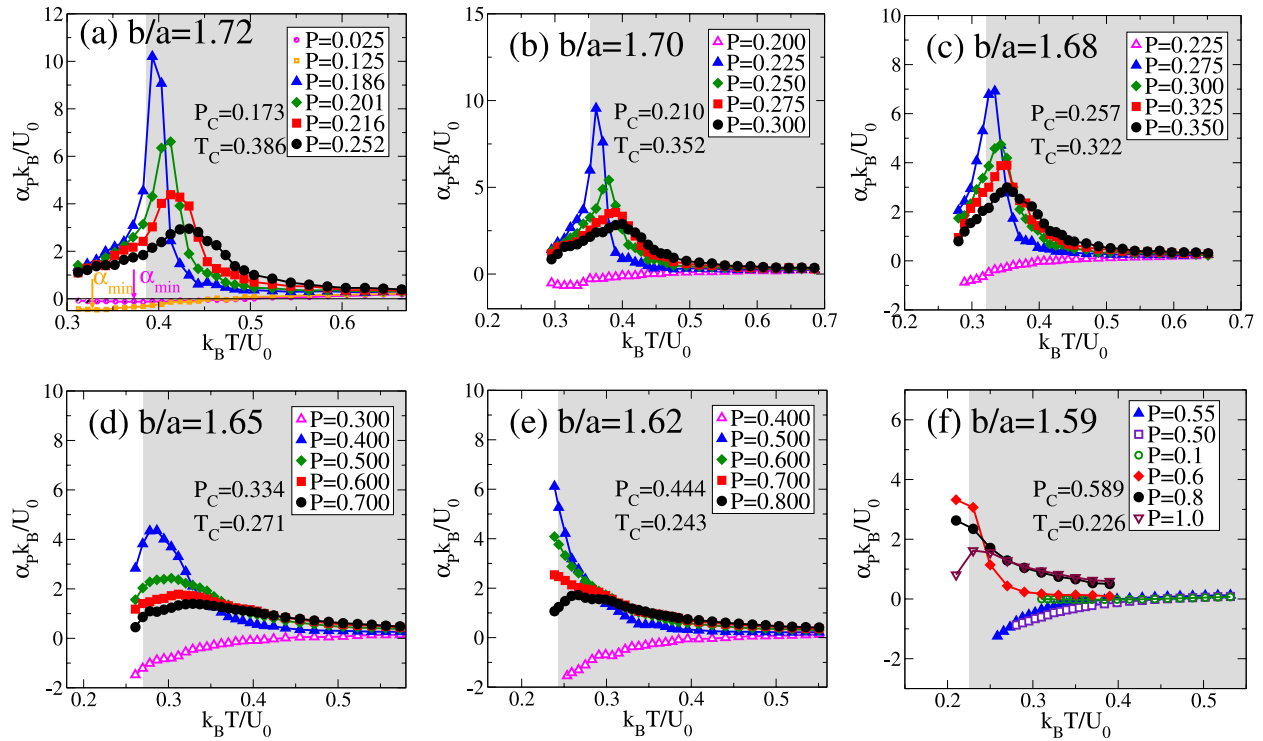


FIG. 7. Thermal expansion, α_P , for models with different b/a . The gray area indicates the $T > T_c$ region. We note that $\alpha_P > 0$ for $P > P_c$ (solid symbols) and $\alpha_P < 0$ for $P < P_c$ (open symbols). ((a)-(e)) For $b/a \geq 1.62$, similar to C_P shown in Figure 3, α_P shows maxima at pressures $P > P_c$, while for pressure $P < P_c$, α_P goes to negative as the temperature drops. The magnitude of α_P monotonically increases as P_c is approached. (f) For $b/a = 1.59$ with horizontal coexistence line, α_P are almost symmetric above and below P_c , with $\alpha_P = 0$ for $P = P_c$. For large P , both the maxima and minima of α_P exist in the equilibrium states (not shown).

maxima line disappears and C_P is no longer an accurate indication of supercritical fluctuations. Indeed, there is no entropy difference between the two coexisting phases, so the critical fluctuations can no longer contribute to entropy fluctuations. However, the density fluctuations remain well defined with two K_T maxima lines associated with the critical fluctuations both above and below the critical pressure. In the vicinity of the critical point, the two K_T maxima lines merge, thus can be used to locate the critical point from measurements obtained in the supercritical region only.

All these results are in good agreement with the linear scaling theory,^{30,44} which predicts that for positively sloped coexistence line, the lines of K_T , α_P , and C_P maxima all converge to the Widom line, which emanates from the critical point into a supercritical region with a positive slope. In particular, the C_P maxima line deviates from the Widom line towards high pressures faster than the line of α_P maxima, which deviates from the Widom line faster than the line of the K_T maxima. When the slope of the coexistence line is horizontal, the linear scaling theory predicts that the line of C_P

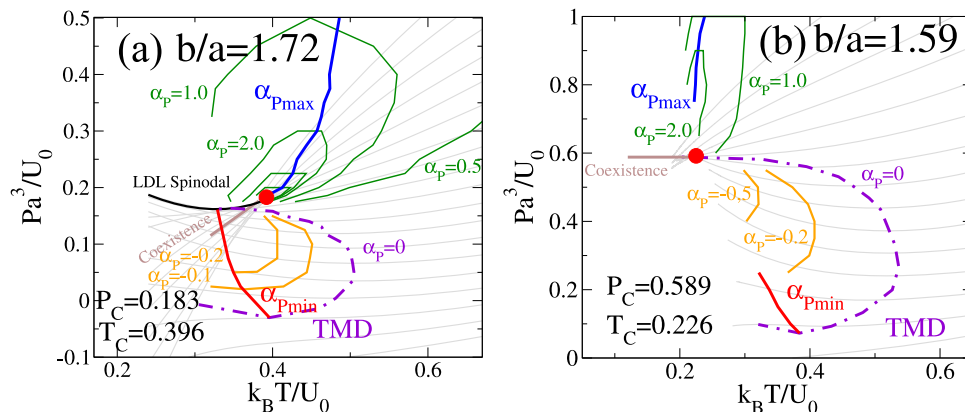


FIG. 8. Lines of equal α_P . (a) For $b/a = 1.72$, the lines of equal α_P ($\alpha_P > 0$ solid green, $\alpha_P < 0$ solid orange) change from $\alpha_P = 1.0$ far away from the LLC to $\alpha_P = 1.0$ close to the LLC with interval $\Delta\alpha_P = 1$ for $P > P_c$, and $\alpha_P = 0$ (TMD) to $\alpha_P = -0.2$ with interval $\Delta\alpha_P = -0.1$ for $P < P_c$. The loci of α_P maxima cross the lines of equal α_P at the points of their maximal pressure and follow the coexistence line into the one-phase region, then sharply turn upwards to higher pressures and become almost vertical. (b) For $b/a = 1.59$, the lines of equal α_P ($\alpha_P > 0$ solid green, $\alpha_P < 0$ solid orange) change from $\alpha_P = 1.0$ far away from the LLC to $\alpha_P = 2.0$ close to the LLC with interval $\Delta\alpha_P = 1.0$ for $P > P_c$, and $\alpha_P = 0$ (TMD) to $\alpha_P = -1.0$ with interval $\Delta\alpha_P = -0.5$ for $P < P_c$.

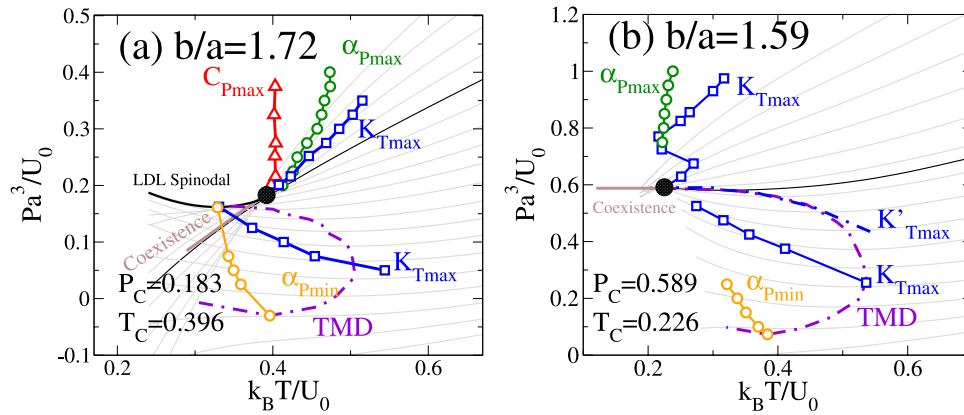


FIG. 9. Phase diagram with specific heat C_P for system ($b/a = 1.72$) with positively sloped coexistence line (a) and for system ($b/a = 1.59$) with horizontal coexistence line (b). Isochores (solid gray), TMD line (dashed purple), and LLCP (large hatched circle) are shown. The critical isochore is marked by a thin black line.

maxima develops two symmetric branches in the subcritical region which merge with the coexistence line in the vicinity of the critical point. Thus, in the vicinity of the critical point with the horizontally sloped coexistence line, C_P does not have maxima as function of temperature at constant pressure for $T > T_c$. In contrast, the lines of K_T maxima symmetrically merge with the Widom line in the supercritical region. The line of α_P maxima for $P > P_c$ merges with the symmetric line of α_P minima for $P < P_c$. Both of these lines deviate from the Widom line, faster than the lines of compressibility maxima.

IV. GLASS TRANSITION

As discussed above [Fig. 2], when the b/a ratio decreases, the LLCP is pushed into a metastable region with respect to crystallization, where the system is close to the GT. Next, we investigate the relationship between LLPT and GT in systems with different coexistence line slopes.

While the inability to equilibrate in this domain was noted by Gibson and Wilding in their seminal study,³⁶ they did not discuss the “glass transition” (which is not a true transition in the thermodynamic sense). The GT is a concept useful for describing the manner in which viscous liquid systems fall out of equilibrium on cooling or regain it during heating. It is better described as a “glass transformation zone” within which the system is neither fully arrested nor fully equilibrated. It may be studied in simulation, as it is in the laboratory,²⁰ by “scanning calorimetry.” In scanning calorimetry, the enthalpy is monitored continuously as the system attempts, and increasingly succeeds, to explore all its degrees of freedom as the temperature rises from low values where all motions except vibrations are frozen out.⁴⁵ Typically, the range of temperature over which the transition extends is the range needed to change the relaxation time by two orders of magnitude, and thus it depends on the temperature-dependence of the relaxation time.⁴⁶ Being kinetic in nature, this transition is hysteretic, as seen in our simulations. While it is usually studied using scanning

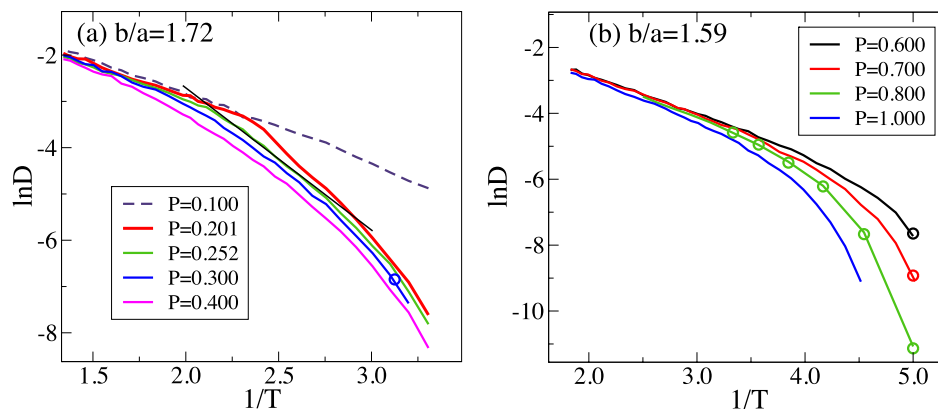


FIG. 10. Arrhenius plot of the diffusivity for different values of b/a . (a) For the case of $b/a = 1.72$, corresponding to the positive slope of the coexistence line, D maintains approximately Arrhenius behavior for the entire range of temperatures for $P < P_c$. This behavior is consistent with very mild increase of C_P upon cooling for $P < P_c$ [Fig. 3]. In contrast, for $P > P_c$, the Arrhenius behavior of D breaks down at the Widom line where the C_P has a sharp maximum. The change of the slope of the Arrhenius plot becomes sharper as P approaches P_c from above. For P close to P_c , we observed that the increase of the slope near the Widom line is followed by its decrease at low temperatures. This behavior is consistent with the fragile-to-strong transition. (b) For the case of $b/a = 1.59$, corresponding to the horizontal slope of the coexistence line, the slope of the Arrhenius plot monotonically increases above P_c , as one would expect for the fragile liquid approaching glass transition. The circles indicate the values of the diffusivity obtained by NVT simulations with the box size equal to the average box size in the NPT simulations at the same pressure. The error bar of the diffusivity obtained by comparing several independent runs at the same T and P is of the order of the circle size.

calorimetry, it can also be studied using volumetric methods. Except in a few anomalous cases like water, the enthalpy and volume are linearly correlated. Even when they are not, the time scales for fluctuations are found to be the same near T_g , a consequence of the cooperativity of molecular relaxation in these conditions.

The glass temperature T_g is defined as the point at which the uptake of configurational enthalpy begins (onset T_g , the value usually reported by experimentalists), or the temperature at which equilibrium (ergodicity) is fully restored, T'_g . Figure 11 shows the diagram defining each one, the distance between the two being approximately 25% of the absolute value. It is a more diffuse phenomenon than in the laboratory where the width is only 5% of the absolute value (due to the increased temperature-dependence of the relaxation time near the laboratory T_g).⁴⁶

As in the laboratory experiment, we estimate T_g and T'_g by plotting the derivative of the enthalpy (the apparent specific heat) during cooling and heating the systems through the GT along isobars slightly above the critical pressure P_c at a constant cooling/heating rate $q_c = q_h = 10^{-6}q_0 \approx 10^9$ K/s [Fig. 11]. We find that for upscans in the positively sloped coexistence line case ($b/a = 1.72$), C_P shows two well-separated peaks [Fig. 11(a)]. The high temperature peak T_W is related to the fluctuations associated with the LLPT and is used to locate the Widom line. The second peak (at the lower temperature $T = T'_g$) is an “overshoot” phenomenon

due to ergodicity restoration kinetics.⁴⁷ It is seen in most laboratory systems (but not polymers) and is not observed during cooling (a measure of the hysteretic character of the glass transition). The lower T_g is obtained from the standard construction (dashed line).⁴⁷

We observe similar widely separated T_W and T'_g peaks for $b/a = 1.70$ and 1.68 [Figs. 11(b) and 11(c)], but the temperature difference between the two peaks shrinks as the b/a value decreases. When $b/a < 1.68$, the “normal” and critical fluctuations merge because of the similarity in their time scales, but study of the density fluctuations as reflected in the compressibility of Fig. 5 shows that indeed $T_c > T_g$, and the critical point is not suppressed by the kinetics of “background” enthalpy fluctuations (as the collected data in Fig. 11 might imply at first sight). The critical fluctuations in enthalpy instead lose their thermodynamic strength because the enthalpy difference between the alternative phases dictated by the Clapeyron equation for horizontal coexistence lines (see Fig. 2 for $b/a = 1.59$) vanishes. This is because a horizontal co-existence line implies by Clapeyron equation, $dp/dT = \Delta S/\Delta V = \Delta H/T\Delta V$ that there is no difference in enthalpy between the two phases in equilibrium, so there will be no anomalous enthalpy fluctuations to diverge as T_c is approached. This does not, however, interfere with the measurement of a glass temperature (Fig. 11) because T_g is reporting the temperature at which the normal enthalpy fluctuations in the liquid are crossing the “experimental” time scale determined by the heating rate. So we can

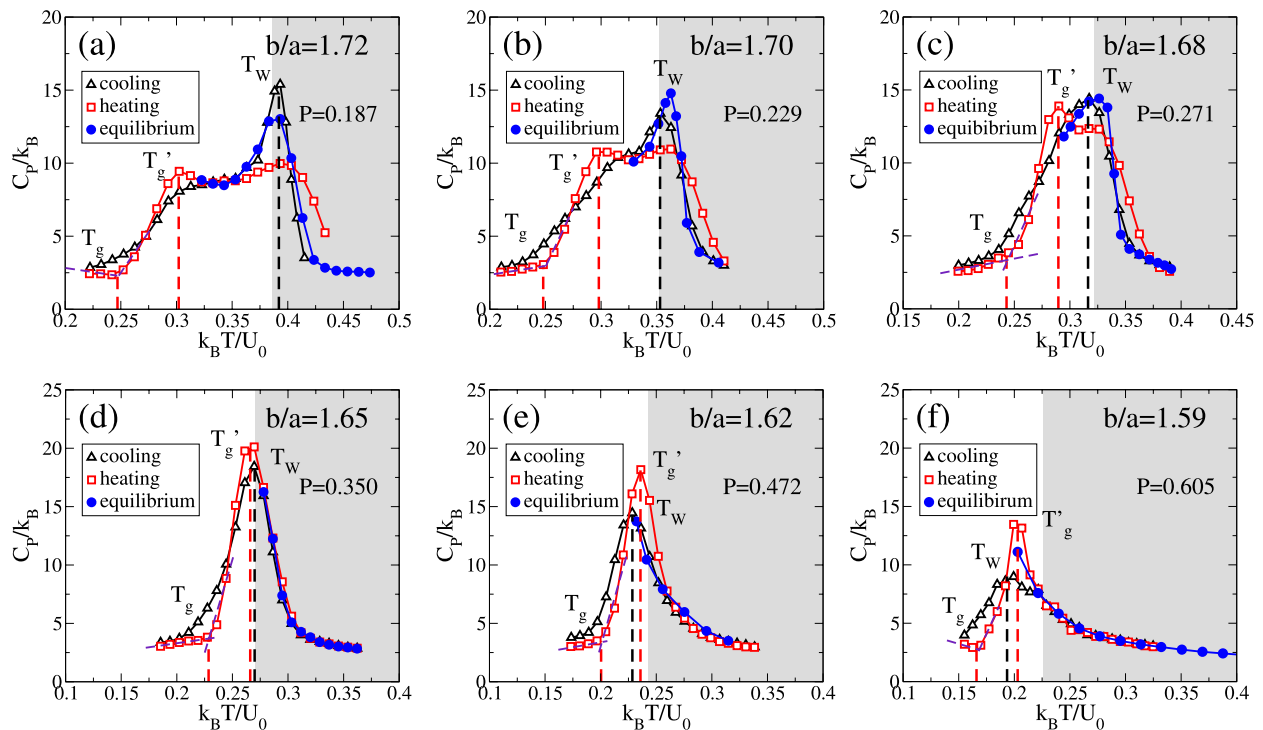


FIG. 11. The comparison of C_P upon slow cooling and heating for a selection of modified Jagla models. ((a)-(c)) For $b/a = 1.72$, 1.70 , and 1.68 , two peaks of C_P upon heating can be observed. The high temperature peak at T_W , arising from the presence of the Widom line, is related to the LLPT. The low temperature peak upon heating at T'_g corresponds to the ergodicity restoration slightly above the glass transition T_g obtained from standard construction (dashed line). One can see that the distance between the glass transition peaks T'_g/T_g and T_W decreases as the b/a value decreases, with the LLCP moving closer to the glass transition. ((d)-(f)) For $b/a = 1.65$, 1.62 , and 1.59 , upon heating, only one peak of C_P can be observed, and this peak shifts below T_c , while for other cases, it is well above T_c . One also notices that system shows a prominent K_T peak in the studied P region (Fig. 5). In these models with small coexistence line slope, the enthalpy fluctuations play less role in the critical fluctuations, while the density fluctuations is the leading term. And as the LLCP being pushed closer to T_g , the critical fluctuations become suppressed by the glass transition, where C_P only shows one peak upon heating.

still see a T_g line even when we cannot see C_p Widom line. Thus, notwithstanding the proximity of the critical point, at $b/a = 1.59$, the apparent specific heat plot is indistinguishable from that previously reported for the glass transition of the low density liquid at pressures well below P_c in the earlier study of Xu *et al.*⁴⁰

Figure 12 shows that the critical fluctuation domain becomes increasingly linked to the slow (glassy) dynamics domain as the repulsive potential becomes steeper (the second length scale closes in on the first length scale as b/a decreases). Unfortunately, the increase in the equilibrium melting point in the same b/a range throws the system into conflict with the faster kinetics of crystal nucleation, and the relation between the first two cannot be followed for smaller b/a .

Just as the mixing of Lennard-Jones (LJ) particles has made possible the study of supercooled and glassy states of LJ particles, so also the mixing of the Jagla particles of different dimensions and attractive well depths makes extended studies of the relationship between the critical point and the glass temperature possible. Note that in the glass-forming LJ mixtures, there is no suggestion of stable domain critical points, although specific heats in excess of vibrational values do increase sharply as temperature decreases.

Note that the strengths of the specific heat and compressibility response functions in laboratory molecular glass-formers also vary in opposite directions as T_g is approached, and that the case of *o*-terphenyl is the best documented so far.⁴⁸ Figures 3 and 5 show that the relationship is similar to that of the maxima of response functions for the present model at

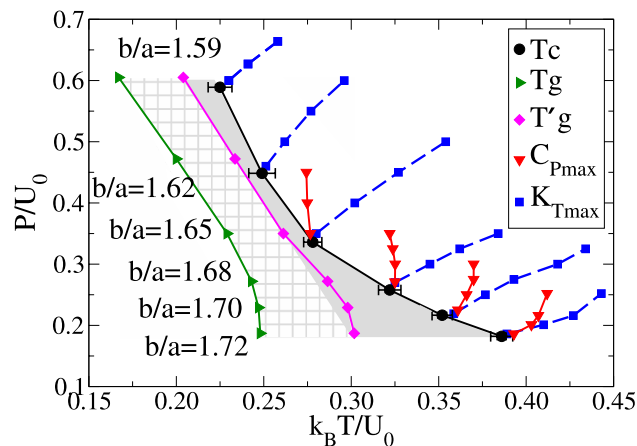


FIG. 12. Relative positions of the glass transition temperature T_g (onset), T'_g (upper limit), critical temperature T_c , and the locus of C_p and K_T maxima near the LLCPC, for models of different b/a . Only the high pressure branch of the K_T maxima locus is shown. The LLCPC shifts to lower temperature and higher pressure as b/a decreases. T'_g follows the same trend of T_c , but the temperature difference (gray area) between T'_g and T_c decreases as b/a decreases. The glass transformation range (between T_g and T'_g) separating glass from liquid is shown (hashed area). For $b/a \leq 1.65$, T_c gets pushed close to T'_g , where in isobaric cooling/heating, only one peak of C_p can be found, instead of two well-separated maxima ($b/a = 1.72 - 1.68$). The locus of C_p maxima increasingly separates from the locus of the K_T maxima with decreasing b/a and is no longer seen for $b/a < 1.65$. The K_T maxima line is a better representative of the Widom line for the case of small and zero sloped coexistence line. T_c lies in the ergodic domain for the b/a studied. For $b/a < 1.59$, the LLCPC cannot be obtained in our study by equilibrium molecular dynamics due to fast crystallization.

small b/a and that there is a temperature interval near the glass transition where C_p increases upon cooling as K_T decreases, the only difference being that there is no stable second critical point in the laboratory case.

V. DISCUSSION AND SUMMARY

We have investigated the loci of the response function maxima in systems with different coexistence line slopes. We find that when the slope of the coexistence line is positive, the C_p maxima line originates at the LLCPC and extends into the one-phase region as a continuation of the coexistence line, and the compressibility K_T exhibits two maxima lines. One of the K_T maxima lines is related to critical fluctuations, originates at the LLCPC, and coincides with the C_p maxima line in the vicinity of the critical point following the Widom line. This allows us to locate the LLCPC from the high temperature side by tracking the C_p maxima line, instead of attempting to track the coexistence line from the low temperature side where crystallization and the glass transition are severe experimental obstacles. The other K_T maxima line approaches the LDL spinodal and terminates at the lowest pressure point of the LDL spinodal, where the TMD line also terminates. For a LLPT with a positive slope of the coexistence line, all response function maxima lines deviate from the critical isochore towards higher pressures as the distance from the LLCPC increases [Fig. 9(a)]. Note that C_p maxima line deviates faster than α_P maxima line which in turn deviates faster than K_T maxima line. This order is in perfect agreement with the predictions of the linear scaling theory³⁰ but differs from the predictions of van der Waals theory and other mean-field theories,^{31,33} which cannot accurately describe the scaling region. The speed of the deviation of the response functions from one another depends on the single fitting parameter of the linear scaling theory a , which defines the scale of the ordering field h_1 . The larger the value of a the closer to the critical point the deviation occurs. Our analysis of the 3d Ising model gives the value of $a = 0.0465$, for the Jagla model, the precise value of a is difficult to determine but it is of the order of unity. Another parameter which determines the speed of the deviation is the slope of the coexistence line: as the slope decreases deviation occurs closer to the critical point.

As the slope of coexistence line approaches zero, the C_p maxima disappear in the equilibrium region with $T \geq T_c$. However, along a constant temperature path, C_p shows a minimum at the critical pressure P_c [Fig. 13]. This is experimentally observed in water in which C_p decreases with increasing pressure.²⁰ Hence, for a system with a horizontal coexistence line, we can still locate the LLCPC using the C_p minimum as a function of P at constant T . For K_T , both of the K_T maxima lines as functions of T are related to critical fluctuations, start at the LLCPC, and extend symmetrically above and below P_c . We can also define a third K_T maxima line as a function of P at constant T (Fig. 6). We can use these three K_T maxima lines that converge at the LLCPC, and the C_p minimum line, to locate the LLCPC. When the slope of the coexistence line is zero, the thermal field coincides approximately with the temperature, and thus this third K_T maxima line gives the best approximation of the Widom line.

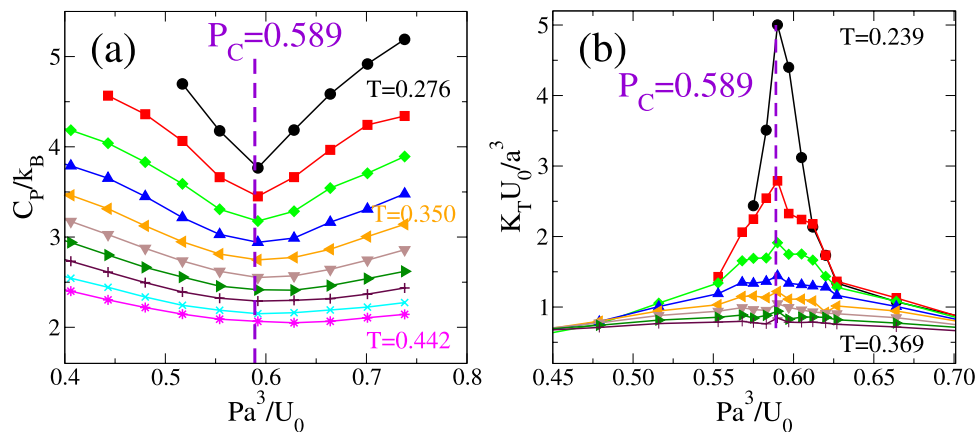


FIG. 13. The behavior of C_P (a) and K_T (b) along different isotherms as functions of P in simulations with a horizontal coexistence line $b/a = 1.59$. (a) T changes from 0.276 to 0.442 with interval $\Delta T = 0.180$, above $T_c = 0.226$. For all temperatures, C_P shows a minimum at P_c and as $T \rightarrow T_c$, the minimum value of C_P increases, and the valley of the minimum gets narrower. This offers a way to track the critical point by isotherms at equilibrium temperatures, instead of isobar cooling into lower temperature. (b) K_T in simulations, T changes from 0.239 to 0.369 with interval $\Delta T = 0.180$, above $T_c = 0.226$. One can see that K_T has maxima at P_c for all temperatures and, as $T \rightarrow T_c$, the maximum value of K_T increases and the peak gets sharper.

When the slope of the coexistence line is negative, the phase diagram near the critical point is the mirror image of the phase diagram for the positive slope of the coexistence line with respect to the critical isobar $P = P_c$. The C_P maxima line and one of the K_T maxima lines both originate at the LLC and extend into the one-phase region, overlapping with each other near the critical point.³⁰ The second K_T maxima line goes above the pressure of the critical point and terminates at the point of maximum pressure of the HDL spinodal, where the TMD line also terminates.

Note that the location of the critical point with respect to the TMD line is related to the slope of the coexistence line. When the slope of the coexistence line is positive, the critical point stays outside the density anomaly region; when it is negative, the critical point is inside the density anomaly region; when it is horizontal, the TMD line terminates at the LLC. Indeed, when the slope is positive, the volume of the low temperature phase is smaller than the volume of the high temperature phase. Thus, if we connect these two phases by the isobar with $P > P_c$, the volume along this isobar decreases with T , the region above the critical point corresponds to the $\alpha_P > 0$ and, because α_P is a continuous function everywhere except at the LLC, α_P also remains positive in the one-phase region for pressure below the LLC. Accordingly, the LLC lies outside the region of density anomaly. Analogous considerations show that, when the slope of the coexistence line is negative, the LLC remains inside the density anomaly region, as is the case for water. We also note that, in all three cases, the two K_T maxima lines at high temperatures, merging with the K_T minima lines, form a loop and cross the TMD line at the point of highest temperature.⁴¹

By changing the parameters of the Jagla interacting potential, we can obtain systems with different slopes of the LLPT coexistence line. We find that, when the slope of the coexistence line is small, the identification of the Widom line is no longer possible by tracing the C_P maxima. As the slope of the coexistence line approaches zero, the C_P maxima lines become increasingly vertical and, when the slope of the coexistence line is horizontal, it cannot be observed in simula-

tions. The study of C_P maxima is best reserved for systems in which the slope of the coexistence line is strongly positive or negative. However, the response function maxima in terms of density fluctuations are still well defined, and it is possible to identify the Widom line by following the loci of K_T maxima. These results are in good agreement with the linear scaling theory.⁴⁴ In the range of this study, the critical point is always located above the (cooling rate dependent) glass temperature T_g , though the two run parallel at lower b/a values.

The family of Jagla models studied here does not produce the LLPT coexistence line with negative slope for any set of studied parameters. A recent study of a continuous core-softened potential similar to the Jagla potential³⁸ shows various response function maxima lines with the negative slopes. However, these lines do not converge to a LLC, and hence cannot be called a Widom line, which by definition exists only in the vicinity of the critical point and is associated with the diverging correlation length. The situation described in Ref. 38 indeed resembles the behavior of the response function maxima in the WAC model of silica¹⁹ in which different response functions achieve global maxima at different points of the $(P - T)$ plane but never diverge. Similar situation exists in a primitive model of tetrahedral interactions.⁴⁹ Hence, the existence of the response function maxima does not necessarily indicate the existence of a critical point. In the latter model, a small change in the parameters of the potential leads to the emergence of the critical point. Accordingly, one can expect that in these models, the line of critical points exists in the three dimensional space formed by pressure, temperature, and some parameter of the model, characterizing the shape of the interaction potential. This line may not cross the $(P - T)$ plane for a given value of this parameter, but its presence affects the response functions in a region of the $(P - T)$ plane around the projection of its endpoint. From the experimentalist point of view, the existence of the response function maxima lines may indicate that a small change in the system, e.g., adding a solute^{50,51} can lead to the emergence of the observable LLPT.

ACKNOWLEDGMENTS

We thank M. A. Anisimov, M. C. Barbosa, D. Corradini, S. Han, and V. T. Holten for helpful discussions. J.L. and H.E.S. thank the NSF Chemistry Division for support (Grant Nos. CHE 0911389 and CHE 0908218). X.L.M. thanks the National Science Foundation of China (Grant Nos. 11174006 and 11290162) and MOST (Grant Nos. 2012CB921404 and 2015CB856800) for support. S.V.B. thanks the Office of the Academic Affairs of Yeshiva University for funding the Yeshiva University high-performance computer cluster and acknowledges the partial support of this research through the Dr. Bernard W. Gamson Computational Science Center at Yeshiva College. C.A.A. acknowledges support from NSF-CHE Grant No. CHE-1213265.

- ¹P. H. Poole, F. Sciortino, U. Essmann, and H. E. Stanley, *Nature* **360**, 324 (1992); *Phys. Rev. E* **48**, 3799 (1993); P. H. Poole, U. Essmann, F. Sciortino, and H. E. Stanley, *ibid.* **48**, 4605 (1993); F. Sciortino, P. H. Poole, U. Essmann, and H. E. Stanley, *ibid.* **55**, 727 (1997).
- ²P. H. Poole, F. Sciortino, T. Grande, H. E. Stanley, and C. A. Angell, *Phys. Rev. Lett.* **73**, 1632 (1994).
- ³L. Xu, P. Kumar, S. V. Buldyrev, S.-H. Chen, P. Poole, F. Sciortino, and H. E. Stanley, *Proc. Natl. Acad. Sci. U. S. A.* **102**, 16807 (2005); G. Franzese and H. E. Stanley, *J. Phys.: Condens. Matter* **19**, 205126 (2007); J. L. F. Abascal and C. Vega, *J. Chem. Phys.* **133**, 234502 (2010); G. G. Simeoni, T. Bryk, F. A. Gorelli *et al.*, *Nat. Phys.* **6**, 503 (2010); P. Kumar, S. V. Buldyrev, S. L. Becker, P. H. Poole, F. W. Starr, and H. E. Stanley, *Proc. Natl. Acad. Sci. U. S. A.* **104**, 9575 (2007); K. T. Wikfeldt, C. Huang, A. Nilsson *et al.*, *J. Chem. Phys.* **134**, 214506 (2011); V. V. Brazhkin, Y. D. Fomin, A. G. Lyapin *et al.*, *J. Phys. Chem. B* **115**, 14112 (2011); P. F. McMillan and H. E. Stanley, *Nat. Phys.* **6**, 479 (2010).
- ⁴Reviews of supercooled and glassy water include: O. Mishima, *Proc. Jpn. Acad., Ser. B* **86**, 165 (2010); C. A. Angell, *Science* **319**, 582 (2008); *Annu. Rev. Phys. Chem.* **55**, 559 (2004); P. G. Debenedetti, *J. Phys.: Condens. Matter* **15**, R1669 (2003); P. G. Debenedetti and H. E. Stanley, *Phys. Today* **56**(6), 40 (2003); O. Mishima and H. E. Stanley, *Nature* **396**, 329 (1998).
- ⁵G. Franzese *et al.*, *Nature* **409**, 692 (2001); G. Malescio *et al.*, *J. Phys.: Condens. Matter* **14**, 2193 (2002); G. Franzese *et al.*, *Phys. Rev. E* **66**, 051206 (2002); G. Franzese, M. I. Marqués, and H. E. Stanley, *ibid.* **67**, 011103 (2003); A. Skibinsky *et al.*, *ibid.* **69**, 061206 (2004); G. Malescio, G. Franzese, A. Skibinsky, S. V. Buldyrev, and H. E. Stanley, *ibid.* **71**, 061504 (2005).
- ⁶V. V. Brazhkin, A. G. Lyapin, S. V. Popova, and R. N. Voloshin, in *New Kinds of Phase Transitions: Transformations in Disordered Substances*, NATO Advanced Research Workshop, Volga River, edited by V. Brazhkin, S. V. Buldyrev, V. Ryzhov, and H. E. Stanley (Kluwer, Dordrecht, 2002), pp. 15–28.
- ⁷D. Paschek, *Phys. Rev. Lett.* **94**, 217802 (2005).
- ⁸M. Yamada, S. Mossa, H. E. Stanley, and F. Sciortino, *Phys. Rev. Lett.* **88**, 195701 (2002).
- ⁹L. Xu and V. Molinero, *J. Phys. Chem. B* **114**, 7320 (2010); **115**, 14210-14216 (2011).
- ¹⁰K. Katayama, T. Mizutani, K. Tsumi, O. Shinomura, and M. Yamakata, *Nature* **403**, 170 (2000); G. Monaco, S. Falconi, W. A. Crichton, and M. Mezouar, *Phys. Rev. Lett.* **90**, 255701 (2003); Y. Katayama, *J. Non-Cryst. Solids* **312**, 8 (2002); Y. Katayama, Y. Inamura, T. Mizutani *et al.*, *Science* **306**, 848 (2004).
- ¹¹H. Bhat, V. Molinero, V. Solomon, E. Soignard, S. Sastry, J. L. Yarger, and C. A. Angell, *Nature* **448**, 787 (2007).
- ¹²H. W. Sheng, H. Z. Liu, Y. Q. Cheng, J. Wen, P. L. Lee, W. K. Luo, S. D. Shastri, and E. Ma, *Nat. Mater.* **6**, 192 (2007).
- ¹³R. Kurita and H. Tanaka, *Science* **306**, 845 (2004).
- ¹⁴S. Sen, S. Gaudio, B. G. Aitken *et al.*, *Phys. Rev. Lett.* **97**, 025504 (2006).
- ¹⁵C. A. Angell, J. Shuppert, and J. C. Tucker, *J. Phys. Chem.* **77**, 3092 (1973).
- ¹⁶R. J. Speedy and C. A. Angell, *J. Chem. Phys.* **65**, 851 (1976).
- ¹⁷Z. Yan, S. V. Buldyrev, N. Giovambattista, and H. E. Stanley, *Phys. Rev. Lett.* **95**, 130604 (2005); Z. Yan, S. V. Buldyrev, N. Giovambattista, P. G. Debenedetti, and H. E. Stanley, *Phys. Rev. E* **73**, 051204 (2006); Z. Yan, S. V. Buldyrev, P. Kumar, N. Giovambattista, P. G. Debenedetti, and H. E. Stanley, *ibid.* **76**, 051201 (2007); Z. Yan, S. V. Buldyrev, P. Kumar, N. Giovambattista, and H. E. Stanley, *ibid.* **77**, 042201 (2008).
- ¹⁸L. Xu *et al.*, *Nat. Phys.* **5**, 565 (2009).
- ¹⁹E. Lascaris, M. Hemmati, S. V. Buldyrev, H. E. Stanley, and C. A. Angell, *J. Chem. Phys.* **140**, 224502 (2014).
- ²⁰H. Kanno and C. A. Angell, *J. Chem. Phys.* **73**, 1940 (1980).
- ²¹K. Amann-Winkel, C. Gainaru, P. H. Handle, M. Seidl, H. Nelson, R. Bohmer, and T. Loerting, *Proc. Natl. Acad. Sci. U. S. A.* **110**, 17720 (2013).
- ²²L. Liu, S.-H. Chen, A. Faraone, C.-W. Yen, and C.-Y. Mou, *Phys. Rev. Lett.* **95**, 117802 (2005); A. Faraone, L. Liu, C.-Y. Mou, C.-W. Yen, and S.-H. Chen, *J. Chem. Phys.* **121**, 10843 (2004).
- ²³P. H. Poole, I. Saika-Voivod, and F. Sciortino, *J. Phys.: Condens. Matter* **17**, L431 (2005).
- ²⁴S. V. Buldyrev, G. Malescio, C. A. Angel, N. Giovambattista, S. Prestipino, F. Saija, H. E. Stanley, and L. Xu, *J. Phys.: Condens. Matter* **21**, 504106 (2009).
- ²⁵S. V. Buldyrev and H. E. Stanley, *Physica A* **330**, 124 (2003).
- ²⁶O. Mishima and H. E. Stanley, *Nature* **392**, 164 (1998); O. Mishima, *Phys. Rev. Lett.* **85**, 334 (2000).
- ²⁷H. E. Stanley, *Rev. Mod. Phys.* **71**, S358 (1999).
- ²⁸J. M. H. Levelt, Ph.D. thesis, University of Amsterdam, Van Gorkum & Co., Assen, The Netherlands, 1958; A. Michels, J. M. H. Levelt, and G. Wolkers, *Physica* **24**, 769 (1958); A. Michels, J. M. H. Levelt, and W. de Graaff, *ibid.* **24**, 659 (1958); M. A. Anisimov, J. V. Sengers, and J. M. H. Levelt Sengers, in *Aqueous System at Elevated Temperatures and Pressures: Physical Chemistry in Water, Steam, and Hydrothermal Solutions*, edited by D. A. Palmer, R. Fernandez-Prini, and A. H. Harvey (Elsevier, Amsterdam, 2004), pp. 29–71.
- ²⁹L. Xu, S. V. Buldyrev, C. A. Angell, and H. E. Stanley, *Phys. Rev. E* **74**, 031108 (2006).
- ³⁰J. Luo, L. Xu, E. Lascaris, H. E. Stanley, and S. V. Buldyrev, *Phys. Rev. Lett.* **112**, 135701 (2014).
- ³¹H.-O. May and P. Mausbach, *Phys. Rev. E* **85**, 031201 (2012).
- ³²G. Ruppeiner, A. Sahay, T. Sarkar, and G. Sengupta, *Phys. Rev. E* **86**, 052103 (2012).
- ³³V. V. Brazhkin, Y. D. Fomin, V. N. Ryzhov, E. E. Tareyeva, and E. N. Tsiok, *Phys. Rev. E* **89**, 042136 (2014).
- ³⁴P. C. Hemmer and G. Stell, *Phys. Rev. Lett.* **24**, 1284 (1970); G. Stell and P. C. Hemmer, *J. Chem. Phys.* **56**, 4274 (1972); J. M. Kincaid and G. Stell, *ibid.* **67**, 420 (1977); J. M. Kincaid, G. Stell, and E. Goldmark, *ibid.* **65**, 2172 (1976); J. M. Kincaid, G. Stell, and C. K. Hall, *ibid.* **65**, 2161 (1976); E. A. Jagla, *ibid.* **111**, 8980 (1999); *J. Phys.: Condens. Matter* **11**, 10251 (1999); *Phys. Rev. E* **63**, 061509 (2001); S. V. Buldyrev *et al.*, *Physica A* **304**, 23 (2002); M. R. Sadr-Lahijany, A. Scala, S. V. Buldyrev, and H. E. Stanley, *Phys. Rev. Lett.* **81**, 4895 (1998); *Phys. Rev. E* **60**, 6714 (1999).
- ³⁵P. Kumar *et al.*, *Phys. Rev. E* **72**, 021501 (2005).
- ³⁶H. M. Gibson and N. B. Wilding, *Phys. Rev. E* **73**, 061507 (2006).
- ³⁷J. Y. Abraham, S. V. Buldyrev, and N. Giovambattista, *J. Phys. Chem. B* **115**, 14229 (2011).
- ³⁸Y. D. Fomin, E. N. Tsiok, and V. N. Ryzhov, *Phys. Rev. E* **87**, 042122 (2013).
- ³⁹H. J. C. Berendsen *et al.*, *J. Chem. Phys.* **81**, 3684 (1984).
- ⁴⁰L. Xu, S. V. Buldyrev, N. Giovambattista, C. A. Angell, and H. E. Stanley, *J. Phys. Chem. B* **130**, 054505 (2009); L. M. Xu *et al.*, *Int. J. Mol. Sci.* **11**, 5185 (2010); L. M. Xu *et al.*, *J. Chem. Phys.* **134**, 064507 (2011).
- ⁴¹S. Sastry, P. G. Debenedetti, F. Sciortino, and H. E. Stanley, *Phys. Rev. E* **53**, 6144 (1996); H. E. Stanley and J. Teixeira, *J. Chem. Phys.* **73**, 3404 (1980).
- ⁴²G. Adams and J. H. Gibbs, *J. Chem. Phys.* **43**, 139 (1965).
- ⁴³F. W. Starr, C. A. Angell, and H. E. Stanley, *Physica A* **323**, 51 (2003).
- ⁴⁴M. A. Anisimov and V. A. Agayan, *Phys. Rev. E* **57**, 582 (1998); D. A. Fuentevilla and M. A. Anisimov, *Phys. Rev. Lett.* **97**, 195702 (2006); V. Holten, C. E. Bertrand, M. A. Anisimov, and J. V. Sengers, *J. Chem. Phys.* **136**, 094507 (2012); C. E. Bertrand and M. A. Anisimov, *J. Phys. Chem. B* **115**, 14099 (2011); V. Holten and M. A. Anisimov, *Sci. Rep.* **2**, 713 (2012).
- ⁴⁵C. A. Angell, *Science* **267**, 1924 (1995); D. Turnbull and M. H. Cohen, *J. Chem. Phys.* **29**, 1049 (1958); M. Goldstein, *ibid.* **64**, 4767 (1976).
- ⁴⁶C. A. Angell and L. M. Torell, *J. Chem. Phys.* **78**, 937 (1983).
- ⁴⁷C. T. Moynihan, A. J. Eastale, J. Wilder, and J. C. Tucker, *J. Phys. Chem.* **78**, 2674 (1974); C. T. Moynihan, A. J. Eastale, M. A. DeBolt, and J. C. Tucker, *J. Am. Ceram. Soc.* **59**, 12 (1976).
- ⁴⁸C. A. Angell and I. Klein, *Nat. Phys.* **7**, 750 (2011).
- ⁴⁹Y. Tu, S. V. Buldyrev, Z. Liu, H. Fang, and H. E. Stanley, *EPL* **97**, 56005 (2012).
- ⁵⁰K. Murata and H. Tanaka, *Nat. Mater.* **11**, 436 (2012).
- ⁵¹J. W. Biddle, V. Holten, and M. A. Anisimov, *J. Chem. Phys.* **141**, 074504 (2014).